Quaternary Science Reviews 29 (2010) 1328–1341

Contents lists available at ScienceDirect

Quaternary Science Reviews

journal homepage: www.elsevier.com/locate/quascirev

Late Quaternary evolution of Reedy Glacier, Antarctica

Claire Todd [a,*], John Stone [a], Howard Conway [a], Brenda Hall [b], Gordon Bromley [b]

[a] Department of Earth and Space Sciences, Box 351310, University of Washington, Seattle, WA 98195, USA
[b] Department of Earth Sciences and the Climate Change Institute, 311 Bryand Global Sciences Center, University of Maine, Orono, ME 04469, USA

ARTICLE INFO

Article history:
Received 5 June 2009
Received in revised form
28 January 2010
Accepted 1 February 2010

ABSTRACT

Fresh deposits above the margins of Reedy Glacier show that maximum ice levels during the last glaciation were several hundred meters above present near the glacier mouth and converged to less than 60 m above the present-day surface at the head of the glacier. Exposure ages of samples from five sites along its margin show that Reedy Glacier and its tributaries thickened asynchronously between 17 and 7 kyr BP At the Quartz Hills, located midway along the glacier, maximum ice levels were reached during the period 17–14 kyr BP. Farther up-glacier the ice surface reached its maximum elevation more recently: 14.7–10.2 kyr BP at the Caloplaca Hills; 9.1–7.7 kyr BP at Mims Spur; and around 7 kyr BP at Hatcher Bluffs. We attribute this time-transgressive behavior to two different processes: At the glacier mouth, growth of grounded ice and subsequent deglaciation in the Ross Sea embayment caused a wave of thickening and then thinning to propagate up-glacier. During the Lateglacial and Holocene, increased snow accumulation on the East Antarctic Ice Sheet caused transient thickening at the head of the glacier. An important result of this work is that moraines deposited along Reedy Glacier during the last ice age cannot be correlated to reconstruct a single glacial maximum longitudinal profile. The profile steepened during deglaciation of the Ross Sea, thinning at the Quartz Hills after 13 kyr BP while thickening upstream. Near its confluence with Mercer Ice Stream, rapid thinning beginning prior to 7–8 kyr BP reduced the level of Reedy Glacier to close to its present level. Thinning over the past 1000 years has lowered the glacier by less than 20 m.

1. Introduction

During the last glacial maximum (LGM) the Antarctic Ice Sheet filled the Ross Sea Embayment. The northern extent of the LGM ice sheet near Coulman Island, and its retreat history during the early Holocene have been established through a combination of marine geophysics and geology (Anderson et al., 1992; Licht et al., 1996; Shipp et al., 1999; Licht and Andrews, 2002), and geologic studies along the coast from Terra Nova Bay south to Hatherton Glacier (Bockheim et al., 1989; Orombelli et al., 1990; Hall and Denton, 2000; Baroni and Hall, 2004; Hall et al., 2004). Conway et al. (1999) applied these data to the model by Stuiver et al. (1981) that compares the retreating ice-sheet grounding line to a 'swinging gate', which swept south along the Transantarctic Mountains (TAM) while remaining pinned north of Roosevelt Island until after 3.2 kyr BP The age control of Conway et al. (1999) raised the possibility that grounding-line retreat was ongoing. Reconstructions of ice thickness in the Ross Sea (e.g., Denton and Hughes, 2002; Huybrechts, 2002) are constrained by measurements of lateral moraines and drift sheets along the margins of outlet glaciers that drain ice from East Antarctica into the Ross Embayment (Oliver, 1964; Mercer, 1968; Mayewski, 1975; Bockheim et al., 1989; Denton et al., 1989). Reedy Glacier is the southernmost of these glaciers. Unlike the outlet glaciers to the north, which now flow into the floating Ross Ice Shelf, Reedy Glacier merges into Mercer Ice Stream upstream from its present-day grounding line in the southeastern Ross Embayment (Fig. 1).

Mercer (1968) mapped lateral deposits of decreasing relative age along the margins of Reedy Glacier, which he termed the Reedy I, Reedy II, and Reedy III drifts. He identified the youngest of these (Reedy III) as dating from the last glacial maximum, based on its unweathered appearance. In order to develop an absolute chronology, fieldwork was conducted on Reedy Glacier during 2003–2004 and 2004–2005. We made glaciological measurements and mapped and sampled glacial deposits, which are described in detail in a companion paper (Bromley et al., 2010). Here, we focus on Reedy III and younger recessional deposits; we will use the terms "last local glacial maximum" and "last glaciation" to describe local changes in the thickness of the glacier which left behind Reedy III

* Corresponding author. Present address: Department of Geosciences, Rieke Science Center, Pacific Lutheran University, Tacoma, WA 98447, USA. Tel.: +1 253 536 5163; fax: +1 253 536 5055.
E-mail address: toddce@plu.edu (C. Todd).

0277-3791/$ – see front matter © 2010 Elsevier Ltd. All rights reserved.
doi:10.1016/j.quascirev.2010.02.001

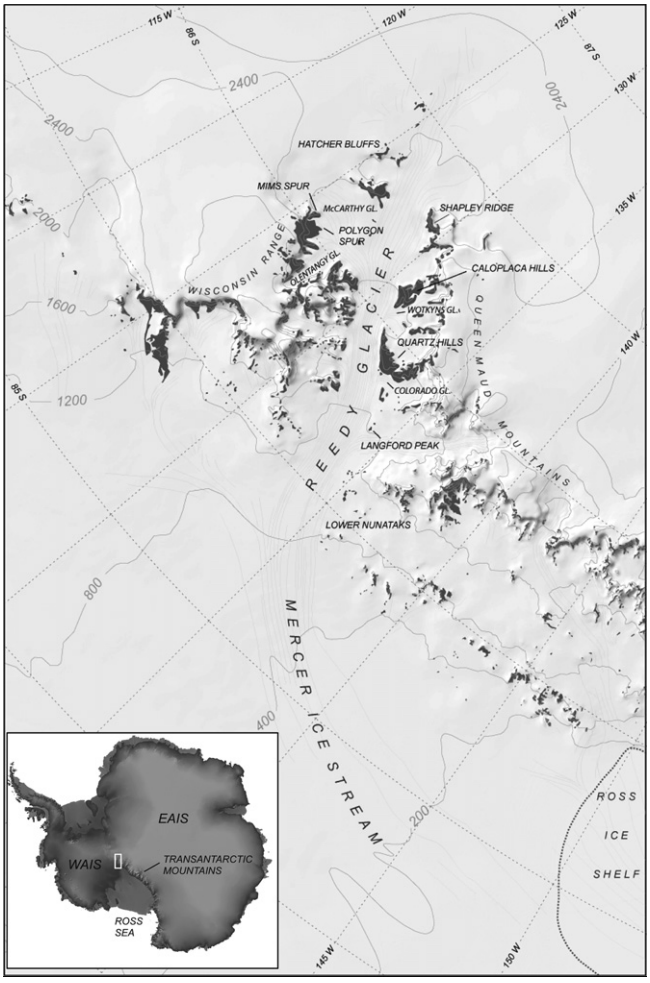

Fig. 1. Area map of Reedy Glacier showing sampling sites, and tributary glaciers. Topography derived from the RAMP-DEM version 2 (Liu et al., 2001). Feature names provided by the Antarctic Digital Database (SCAR, 2002), and USGS topographic maps. Graphics by Dr. Greg Balco.

deposits. We present exposure ages based on cosmic ray produced ^{10}Be in glacial erratics, and use these ages to track the evolution of the glacier surface profile over the past ~17 kyr. We relate the ice-thickness history of Reedy Glacier to the growth and retreat of the Ross Sea ice sheet in the Ross Embayment downstream, and the East Antarctic Ice Sheet upstream. In addition, our results indicate that grounding-line retreat in this sector of the WAIS had substantially slowed by ~1 kyr BP.

2. Regional setting

2.1. Glaciology

Reedy Glacier originates from the polar plateau (86.5°S, 126°W) at nearly 2000 m above sea level (asl) and flows northward 140 km, where it emerges from the TAM at ~600 m asl as the main tributary of Mercer Ice Stream (Fig. 1). The glacier is flanked by the Wisconsin Range to the east and by the Queen Maud Mountains to the west. The RAMP digital elevation database (Liu et al., 2001) indicates that the glacier catchment covers σ25,000 km^2 of the polar plateau. Ice-surface velocities derived from repeat survey of poles set across the glacier at the Quartz Hills (~13 months between measurements) using the Global Positioning System (GPS) indicate a center-line velocity of ~170 m/yr, which is consistent with values derived from InSAR data (Joughin and Tulaczyk, 2002). Our ground-based radar measurements across the glacier at the Quartz Hills indicate the ice there is as much as 2 km thick; bed-elevation near the middle of the glacier is about 850 m below sea level. Present-day ice flux is ~2 km^3/yr.

Reedy Glacier has several tributaries (Fig. 1), but their geometry and flow rates indicate that their contribution to the overall ice flux is small. For example, repeat GPS measurements of a survey pole in Colorado Glacier indicate little or no ice-flow toward Reedy Glacier, and a point radar measurement on Wotkyns Glacier indicates that the ice-thickness is less than 750 m.

Surface mass balance varies along the glacier. In the upper reaches of the glacier the mass balance is positive, but pole measurements across the glacier in the blue-ice region near the Quartz Hills indicate ablation of 0.19–0.25 m/yr ice equivalent (~13 months between measurements). Surprisingly, this is similar to the ablation rate measured at similar elevations on blue-ice areas of Taylor Glacier more than 1200 km to the northwest (Robinson, 1984; Kavanaugh et al., 2009).

2.2. Glacial deposits

Glacial deposits consisting of both rounded basal and angular surficial material are common adjacent to Reedy Glacier (see Bromley et al., 2010). Near the head of the glacier, deposits are thin and sparse, typically consisting of isolated cobbles and boulders lodged on the slopes of protruding nunataks (Fig. 2). We infer that basal clasts become lodged as ice flows up and around such obstructions and are exposed when the glacier thins. On the tip of Mims Spur (Fig. 1), a 2 m-high ice-cored lateral moraine marks the upper limit of ice thickening (Fig. 2).

Down-glacier at the confluence of Colorado and Reedy Glaciers, an ice-cored medial moraine composed of fresh cobbles and boulders has formed by sublimation (Fig. 3). The source of debris is an ablation field on the ice surface at the foot of the Quartz Hills. Till accumulated in this way can become stranded on the underlying topography if the glacier thins, leaving draped, ice-cored deposits on the hill slopes. Such deposits are typical of Reedy III drift, particularly in the Quartz Hills. Erratics originating from ablation till will yield surface-exposure ages that pre-date their eventual deposition. The difference between exposure and depositional ages can be significant when the ice surface maintains a stable elevation for a period of time; during periods of deglaciation the difference will be smaller. The range of ages in such deposits provides limiting constraints on the timing and duration of periods of stability, and on rates of thinning during deglaciation.

During its last expansion Reedy Glacier was much wider at its mouth and overran all of the low nunataks on its western margin (Fig. 1), as indicated by the presence of recessional drift on these peaks. This drift is concentrated on the lower slopes of the peaks and extends on to ice-surfaces upstream from them in several places. We distinguish three types of debris accumulations (Fig. 4): (1) Supraglacial till covering blue-ice ablation patches between and adjacent to the nunataks. These "drifting moraines" (Chinn, 1994) contain rock that has not yet been deposited; exposure ages of cobbles from two of these ablation fields range from 130 to 320 (±30–50) years (discussed below). (2) Drapes of till covering low-elevation nunataks formed when ablation till of type 1 became stranded as underlying ice thinned. (3) Sparsely scattered, unweathered erratics on bedrock or older till cover near the summits of nunataks. We infer that these erratics are lodged at the glacier bed, and uncovered during recession. We cannot rule out the possibility that they also originated as supraglacial ablation till (i.e., type 1), but the sparsity of debris contrasts with modern examples of blue-ice ablation till in the region (compare Fig. 4B and

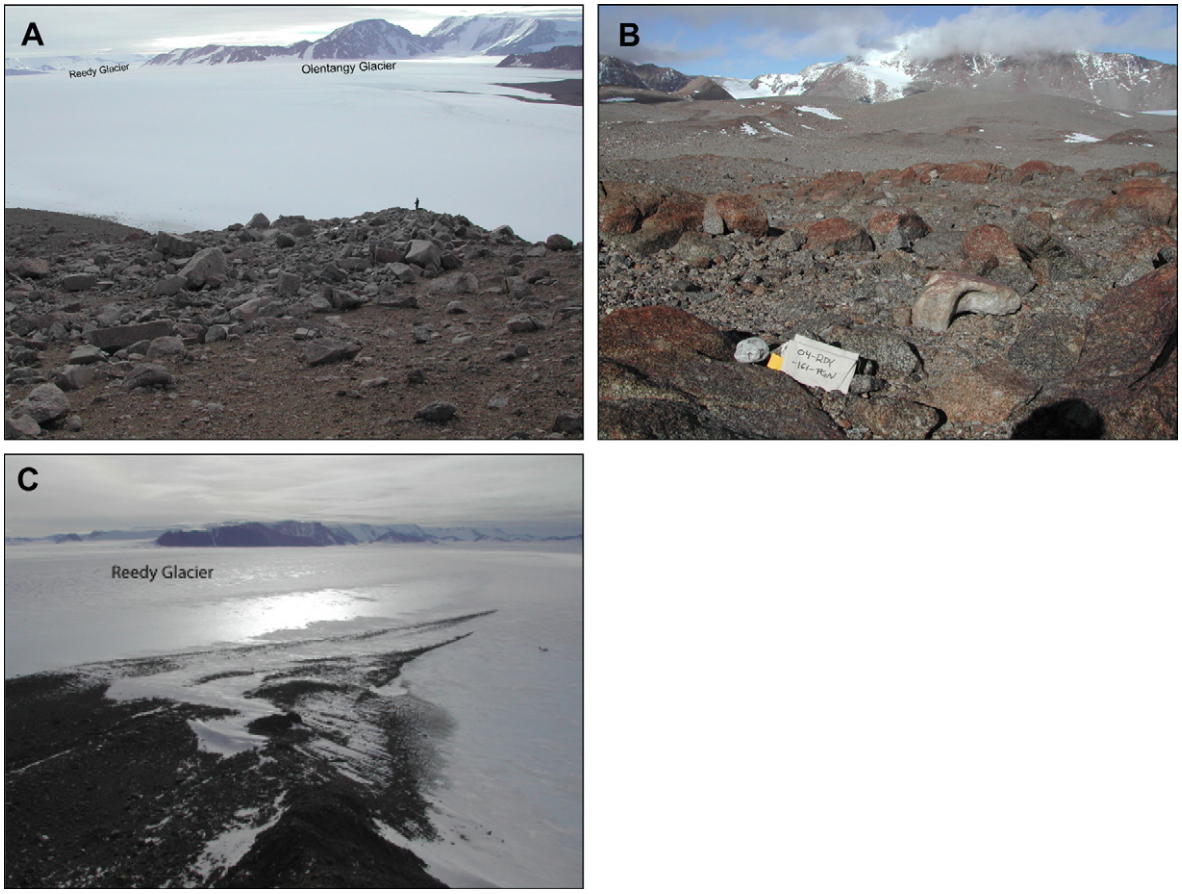

Fig. 2. Glacial deposits found near the head of Reedy Glacier. A) Ice-cored moraine (1920 m asl) at Mims Spur, facing northwest. B) Erratic in sparse Reedy III deposit on a broad bedrock bench at Polygon Spur. C) Northwest-facing image of till-covered ablation area at Hatcher Bluffs near the head of Reedy Glacier. Reedy Glacier flows toward the upper right corner of the photograph and is ~15 km wide in this location.

C). The concentration of ablation till on the ice around and between nunataks, and its absence on the fast-flowing glacier surface, suggests that it begins to accumulate mostly after nunataks emerge, pinning flow and producing areas of rapidly subliming, slow-flowing ice (Chinn, 1994).

3. Methods

3.1. Glacial geologic mapping

Bromley et al. (2010) mapped the distribution, elevation, morphology, and geometry of moraines, drift sheets, erratics, and glacial erosional features on enlarged vertical aerial photographs with a scale of 1:20,000. At least eight major drift units were identified based on characterization of drift stratigraphy, sedimentology, lithology and weathering characteristics of clast populations. As discussed above, deposits from the most recent glaciation and subsequent recession generally consist of fresh ice-cored (or formerly ice-cored) till that overlies bedrock or older weathered till surfaces. Exposure dating of erratics from these deposits (see below) confirms the drift boundaries delineated by glacial geologic mapping.

3.2. Exposure dating

We dated Reedy III deposits using established cosmogenic nuclide methods (e.g., Brown et al., 1991; Lal, 1991; Nishiizumi et al., 1991; Gosse and Phillips, 2001; Balco et al., 2008). Exposure dating in Antarctica is complicated by (i) recycling of material from old deposits into younger moraines, (ii) the ability of cold-based glacier margins to advance over existing drift with little disturbance, and (iii) the need to distinguish between sub-glacially derived clasts suitable for dating, and supraglacial material that may have been exposed to cosmic rays at its source. In addition, disturbance by periglacial activity or collapse of ice-cored moraines after deposition can overturn or bury and exhume samples, leading to underestimation of exposure ages (Stone et al., 2003; Sugden et al., 2005; Ackert et al., 2007). In order to minimize these effects we collected the freshest possible erratics resting stably on bedrock, or on compacted pavements from previous glaciations, or perched on large boulders. In addition, we collected and processed a large number of samples from each site in order to be able to detect consistent ages or trends in age with elevation. Samples were collected over two field seasons in 2003–2004 and 2004–2005. Topographic map elevations are unreliable in the field area, so relative elevations were measured with a high-precision digital barometer (reading to ±0.1 m). These were converted to altitude by calibration to campsite and waypoint altitudes measured with a dual-phase geodetic GPS receiver. Overall accuracy in altitudes is typically ±3–4 m, based on repeat measurements. Shielding due to surrounding topography was measured from digital fisheye photographs (184° field of view) at each site.

In preparation for ^{10}Be analysis, we separated quartz using heavy liquids and by etching samples with dilute hydrofluoric acid (Kohl and Nishiizumi, 1992). We extracted ^{10}Be from quartz using a procedure developed by Ditchburn and Whitehead (1994; see

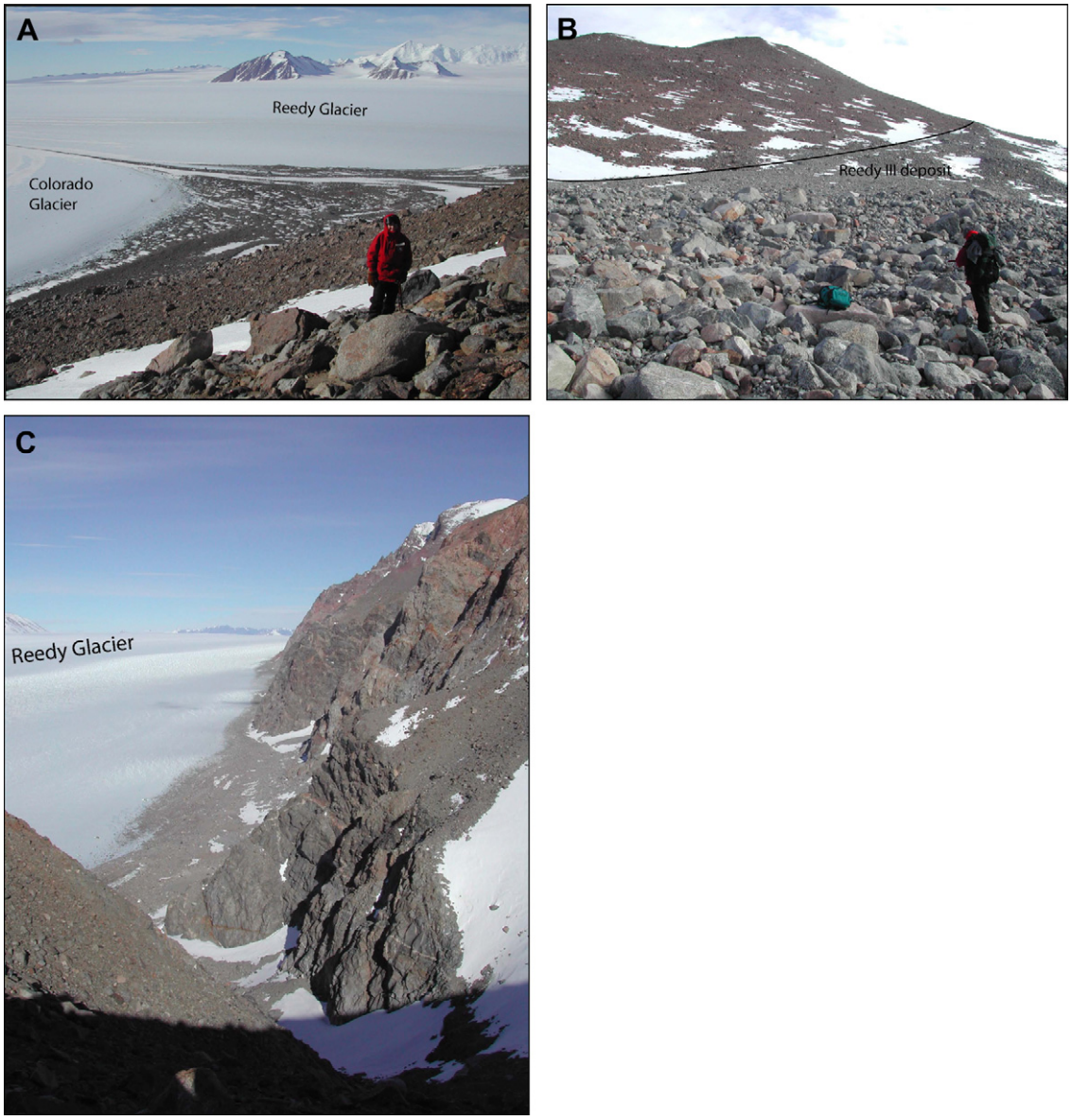

Fig. 3. Glacial deposits found in the Quartz Hills, Reedy Glacier. A) Till-covered blue-ice ablation area at the confluence of Reedy and Colorado Glaciers, facing roughly northeast. Reedy Glacier is ~10 km wide in this location. B) Upper limit of the Reedy III deposit in the Quartz Hills, ~1400 m asl. The margin of relatively unweathered, gray, Reedy III till is visible in the foreground. In contrast, the older, more weathered Reedy II deposit is visible in the background. C) Reedy III deposit in a south-facing gully in the Quartz Hills. Reedy Glacier flows to the left margin of the photograph.

also Stone et al., 2001). Isotope ratios were measured at the Lawrence Livermore National Laboratory Center for Accelerator Mass Spectrometry (LLNL-CAMS) and Purdue Rare Isotope Measurement Laboratory (PRIME Lab). Exposure ages for 93 samples (Tables 1–3) was calculated using version 2.1 of the CRONUS calculator (Balco et al., 2008). Uncertainties shown in the tables are based on fully propagated measurement errors and uncertainties in calibration of the Be-10 production rates. They do not include possible systematic errors in production rates which might result from changing air pressure at the sites, either due to climatic changes or isostatic rebound (e.g., Stone, 2000; Staiger et al., 2007).

4. Results

We dated the upper limit of Reedy III deposits at four locations along the margin of the glacier and its tributaries (Hatcher Bluffs, Mims Spur, Caloplaca Hills, Quartz Hills). Nunataks and peaks down-glacier from the Quartz Hills all were overrun during this maximum; thus, there is no record of the last glacial maximum limit for the lower half of the glacier. Our results show that Reedy Glacier and its tributaries reached maximum ice thickness at different times at different locations on the glacier. Post-glacial thinning was dated using exposure ages of erratics located at elevations below the upper limit of the Reedy III deposits at five locations (Hatcher Bluffs, Mims Spur, Polygon Spur, Quartz Hills, and lower Reedy Glacier). Exposure ages are presented in Tables 1–3.

4.1. Surface-exposure ages of the upper limit of Reedy III deposits

4.1.1. Quartz Hills

The Reedy III deposit at the Quartz Hills is an ablation till that covers part of a broad bench above the confluence of Reedy and Colorado Glaciers (Fig. 5, Bromley et al., 2010). The deposit consists of up to 30 cm of sand and cobbles, plus larger boulders, overlying an

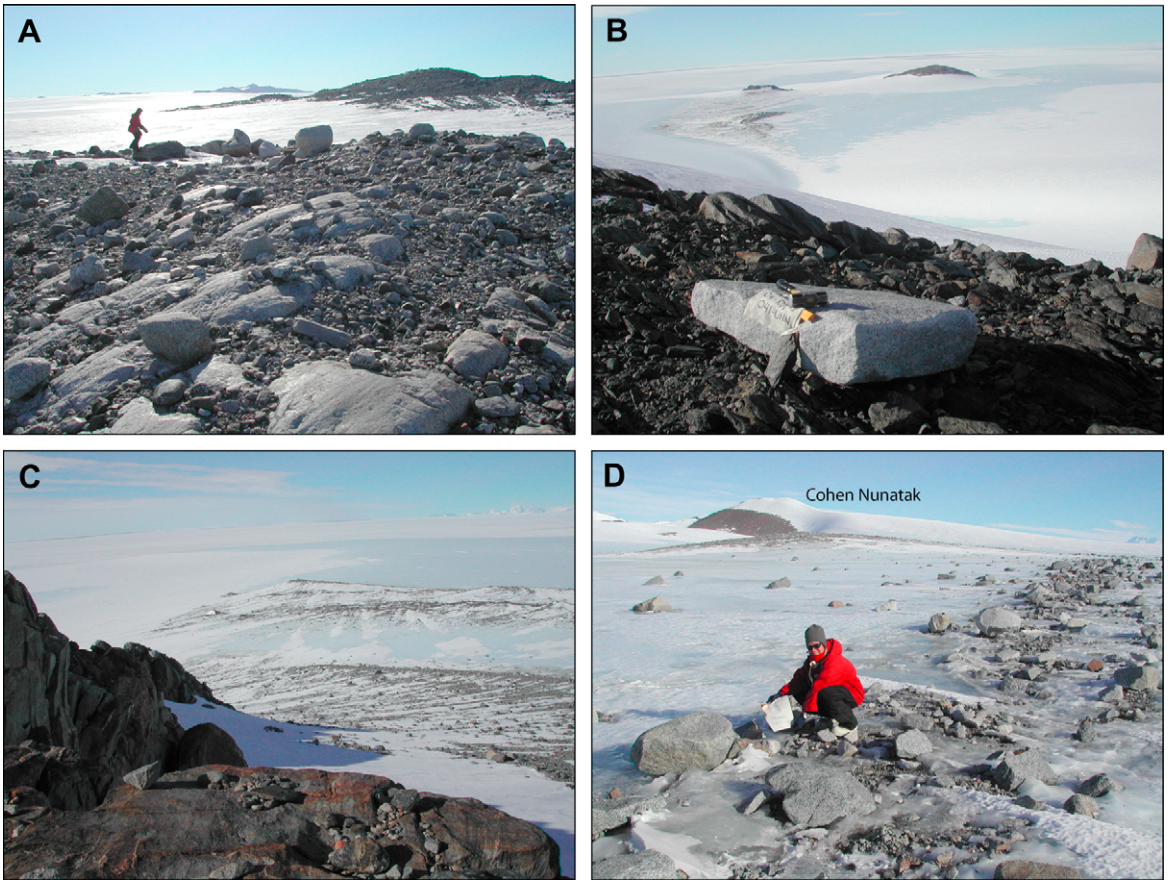

Fig. 4. Glacial deposits found near the mouth of Reedy Glacier. A) Drape deposit covering a recently emerged nunatak (730 m asl). B) Glacial erratic on the summit of Pip's Peak (*informal name*, 893 m asl), facing roughly east. Reedy Glacier flows to the left, beyond the low nunataks in the mid-ground of the photograph. C) "Drifting moraine" in a blue-ice ablation area (630 m asl) at the foot of Cohen Nunatak, at the mouth of Reedy Glacier, facing roughly northeast. Reedy Glacier flows to the northwest through the mid-ground of the photograph. D) Close up of the "drifting moraine" deposit shown in C.

ice core several meters thick. However, near the edge of the bench it thins and erratics are scattered across an older, compacted till surface. The elevation of the upper Reedy III limit ranges from 1410 to 1360 m, roughly 210–250 m above the modern glacier surface. Today at the confluence, a medial moraine originates in a large till-covered, blue-ice ablation area at the foot of the Quartz Hills (Fig. 3A). The extent and lithology of the ablation till on the bench above the confluence suggests that an analogous deposit existed during the last glaciation. Six of twelve surface-exposure ages from the upper limit of this deposit yield a weighted mean of 16.0 ± 0.2 kyr BP, and range from 17.0 ± 1.5 kyr BP to 14.1 ± 1.3 kyr BP (Table 1, Figs. 5 and 6). We attribute this range to exposure in an ablation field similar to the one found at the base of the Quartz Hills today. This interpretation suggests that maximum ice thickness persisted for at least ~3 kyr, lasting from 17.0 ± 1.5 kyr BP or earlier to 14.1 ± 1.5 kyr BP or later (Table 1, Figs. 5 and 6). Six additional samples with exposure ages ranging from 93 to 33 kyr BP likely reflect prior exposure, either in the Quartz Hills or at another location up-glacier. The extent and thickness of this deposit also suggests that much of the material was present in the Quartz Hills prior to ice advance, and was simply reworked *in situ*.

4.1.2. Caloplaca Hills

The Reedy III deposit at the Caloplaca Hills indicates that ice from the tributary Wotkyns Glacier flowed southward into a valley parallel to Reedy Glacier (Fig. 7; Bromley et al., 2010). The upper limit is marked by fresh erratics perched on top of weathered, embedded boulders (Fig. 7). Exposure ages of four of these erratics yield a weighted mean of 11.6 ± 0.2 kyr BP, and range from 14.7 ± 1.3 kyr BP to 10.2 ± 1.0 kyr BP (Table 2, Fig. 8). Possible explanations for this range of ages include (1) multiple ice advances, or (2) a sustained maximum thickness of Wotkyns Glacier beginning before 14.7 ± 1.3 kyr BP and remaining at this maximum elevation until 10.2 ± 1.0 kyr BP or later. The spread in ages down to values younger than the age of the Reedy III limit at Quartz Hills is not due to disturbance, burial or overturning of the samples, which come from both large stable blocks and cobbles perched on top of similar blocks (Fig. 7). Neither the morphology of the deposit nor the location of the young *vs*. old samples suggests that they were laid down in separate advances. The oldest age, 14.7 ± 1.3 kyr BP, coincides with the highstand of the glacier at Quartz Hills, but the younger ages, around 10.3 kyr BP, postdate the onset of thinning there. We conclude that Wotkyns and Reedy Glaciers thickened synchronously, but Wotkyns and upper Reedy Glacier at Caloplaca Hills remained close to their maximum thickness after the onset of deglaciation at Quartz Hills. Five samples with exposure ages ranging from 117 to 25 kyr BP (Table 2, Fig. 8) are significantly older than the cluster of four younger ages. Thus, we interpret these as evidence of prior exposure either locally or farther up-glacier.

4.1.3. Mims Spur

Mims Spur descends from the Wisconsin Plateau along the northern margin of McCarthy Glacier toward its confluence with

Table 1
Surface-exposure ages from the Quartz Hills, Reedy Glacier.

Sample	Latitude (deg S)	Longitude (deg W)	Altitude (m asl)	Thickness correction	Horizon correction	[Be-10][a] (10^4 atom/g)	Exposure age[b] (kyr)	Range[c] (kyr)
Reedy III limit (glacial maximum deposits; W to E)								
03-RDY-005-QZH	*85.90023*	*132.78708*	*1403*	*0.970*	*0.989*	*71.8 ± 1.5*	*32.7 ± 2.9 (0.7)*	*32.2–34.4*
03-RDY-007-QZH	85.90123	132.75317	1401	0.941	0.991	30.3 ± 0.7	14.1 ± 1.3 (0.3)	14.0–14.9
03-RDY-008-QZH	*85.90123*	*132.75317*	*1400*	*0.945*	*0.991*	*123.7 ± 2.4*	*58.0 ± 5.2 (1.1)*	*57.0–61.1*
03-RDY-009-QZH	85.90322	132.69650	1363	0.929	0.983	31.9 ± 0.7	15.6 ± 1.4 (0.4)	15.5–16.5
03-RDY-021-QZH	*85.90260*	*132.69640*	*1353*	*0.949*	*0.989*	*68.8 ± 1.9*	*33.3 ± 3.1 (0.9)*	*32.9–35.1*
03-RDY-019-QZH	85.90360	132.68273	1359	0.929	0.990	33.7 ± 1	16.5 ± 1.5 (0.5)	16.4–17.4
03-RDY-024-QZH	85.90448	132.54638	1391	0.933	0.999	36.3 ± 0.9	17.0 ± 1.5 (0.4)	16.9–17.9
03-RDY-025-QZH	*85.90448*	*132.54638*	*1391*	*0.949*	*0.999*	*115.4 ± 2.2*	*53.8 ± 4.8 (1.1)*	*53.0–56.7*
03-RDY-026-QZH	*85.90453*	*132.51820*	*1392*	*0.953*	*0.999*	*130.1 ± 1.9*	*60.5 ± 5.4 (0.9)*	*59.5–63.7*
03-RDY-027-QZH	85.90453	132.49523	1399	0.937	0.989	32.8 ± 0.8	15.4 ± 1.4 (0.4)	15.3–16.2
03-RDY-077-QZH	85.90452	132.49380	1390	0.957	0.989	35.3 ± 0.7	16.4 ± 1.5 (0.3)	16.2–17.2
03-RDY-028-QZH	*85.90452*	*132.49345*	*1394*	*0.943*	*0.989*	*195.1 ± 2.7*	*93.1 ± 8.4 (1.3)*	*91.4–98.1*
Weighted mean of samples with a simple exposure history							16.0 ± 0.2	
Recessional deposits below Reedy III deposit on Quartz Hills bench (by altitude)								
03-RDY-056-QZH	85.89955	132.57832	1310	0.945	0.999	26.6 ± 0.8	13.2 ± 1.2 (0.4)	13.1–13.9
03-RDY-057-QZH	85.89955	132.57832	1310	0.941	0.999	17.9 ± 1.4	8.9 ± 1.0 (0.7)	8.9–9.4
03-RDY-058-QZH	85.89955	132.57832	1310	0.925	0.999	19.3 ± 0.5	9.7 ± 0.9 (0.2)	9.7–10.3
03-RDY-055-QZH	85.89935	132.58710	1309	0.921	0.999	26.4 ± 0.6	13.4 ± 1.2 (0.3)	13.4–14.1
03-RDY-048-QZH	85.89832	132.59722	1302	0.974	0.999	16.7 ± 0.4	8.1 ± 0.7 (0.2)	8.1–8.6
03-RDY-045-QZH	85.89838	132.59863	1296	0.957	0.998	20.2 ± 0.5	10.0 ± 0.9 (0.2)	10.0–10.6
03-RDY-046-QZH	85.89838	132.59863	1296	0.949	0.999	28.8 ± 0.5	14.4 ± 1.3 (0.3)	14.3–15.2
03-RDY-053-QZH	*85.89878*	*132.59013*	*1294*	*0.941*	*0.998*	*480 ± 8*	*256 ± 24 (5)*	*252–271*
03-RDY-050-QZH	*85.89867*	*132.58910*	*1293*	*0.949*	*0.998*	*70.2 ± 1.2*	*35.3 ± 3.1 (0.6)*	*35.0–37.3*
03-RDY-052-QZH	85.89867	132.58910	1293	0.941	0.998	20.8 ± 0.6	10.5 ± 1.0 (0.3)	10.5–11.1
03-RDY-052-QZH_RPT	85.89867	132.58910	1293	0.941	0.998	20.2 ± 0.7	10.2 ± 1.0 (0.4)	10.2–10.8
03-RDY-033-QZH	85.89733	132.60530	1290	0.974	0.998	19.5 ± 0.5	9.5 ± 0.9 (0.2)	9.5–10.1
03-RDY-036-QZH	*85.89753*	*132.60825*	*1282*	*0.949*	*0.998*	*100.3 ± 1.9*	*51.1 ± 4.6 (1.0)*	*50.6–54.0*
03-RDY-037-QZH	85.89753	132.60825	1282	0.957	0.998	15.1 ± 0.4	7.6 ± 0.7 (0.2)	7.5–8.0
03-RDY-032-QZH	85.89758	132.61042	1280	0.933	0.998	28.9 ± 0.7	14.9 ± 1.3 (0.3)	14.9–15.7
03-RDY-030-QZH	85.89788	132.61377	1280	0.933	0.998	23.5 ± 0.6	12.1 ± 1.1 (0.3)	12.1–12.8
03-RDY-029-QZH	85.89803	132.61128	1276	0.961	0.997	16 ± 0.9	8.0 ± 0.8 (0.5)	8.0–8.5
03-RDY-038-QZH	85.89690	132.62010	1272	0.945	0.998	13.8 ± 0.8	7.0 ± 0.7 (0.4)	7.0–7.4
03-RDY-041-QZH	*85.89717*	*132.61902*	*1266*	*0.953*	*0.998*	*493 ± 9*	*266 ± 25 (5)*	*262–283*
03-RDY-042-QZH	85.89627	132.63007	1246	0.953	0.998	17.4 ± 1.3	9.0 ± 1.0 (0.7)	9.0–9.5
03-RDY-043-QZH	85.89627	132.63007	1246	0.949	0.998	19.9 ± 1.1	10.3 ± 1.1 (0.5)	10.3–10.9
Recessional deposits on bluff overlooking glacier (by altitude)								
04-RDY-105-QZHL	85.91008	132.34532	1310	0.941	0.955	21.7 ± 0.8	11.3 ± 1.1 (0.4)	11.3–11.9
04-RDY-104-QZHL	85.91013	132.34377	1304	0.925	0.939	12.6 ± 0.6	6.8 ± 0.7 (0.3)	6.7–7.1
04-RDY-102-QZHL	*85.90997*	*132.34222*	*1284*	*0.929*	*0.868*	*67.1 ± 1.7*	*39.8 ± 3.6 (1.0)*	*39.4–42.1*
04-RDY-103-QZHL	85.90997	132.34222	1284	0.929	0.852	27.2 ± 1	16.4 ± 1.6 (0.6)	16.3–17.3

Italics indicate samples assumed to have a complex exposure history.
Full CRONUS calculator input data for checking/recalculation of these results archived at: http://depts.washington.edu/cosmolab/data/.
[a] Be-10 concentrations based on Be isotopic measurements normalized to pre-2007 values of the KNSTD standard series. Multiply by 1.106 for values compatible with post-2007 normalization. See Nishiizumi et al. (2007).
[b] Simple exposure age assuming steady production rate; altitude corrections per Lal (1991) as implemented in the CRONUS calculator (http://hess.ess.washington.edu/math/). Uncertainties are external errors including all known analytical and production rate contributions propagated at the $\pm 1\sigma$ level. Values in parentheses are internal errors, which do not include contributions to uncertainty in the final exposure ages common to all samples, such as production rate and scaling errors. External errors should be used when comparing these ages to ages obtained with other dating methods. Internal errors should be used to assess the consistency of exposure ages at a given site.
[c] Range of exposure ages returned by the four paleomagnetically corrected production rate scaling methods implemented in the CRONUS calculator. As noted in (b) above, these ranges are appropriate for external comparisons with other dating methods, and should not be used to assess the internal consistency of ages from a given site.

Olentangy Glacier (Fig. 1.). The area, along with adjacent Polygon Spur, is ~20 km upstream from the junction of Olentangy Glacier with Reedy Glacier. The Reedy III drift limit, which closely parallels the McCarthy Glacier margin today, decreases from 2034 m to 1936 m across the face of Mims Spur, ~140 m higher than McCarthy Glacier (Fig. 9, Bromley et al., 2010). At its south end, the upper limit of the Reedy III deposit is marked by a faint alignment of fresh boulders and cobbles; down-glacier the density of erratics increases and develops into a 2-m-high ice-cored moraine running across the north ridge of Mims Spur (Fig. 2). Six surface-exposure ages from this moraine yield a weighted mean of 8.6 ± 0.1 kyr BP, and range from 9.1 ± 0.9 kyr BP to 7.7 ± 0.7 kyr BP Although our samples include both perched cobbles and large boulders, this range of ages could be attributed to gradual degradation of the ice-cored moraine. It is also possible that McCarthy Glacier reached a maximum thickness by 9.1 ± 0.9 kyr BP, and remained close to this maximum elevation until 7.7 ± 0.7 kyr BP (Table 2, Fig. 10). We can neither prove nor rule out either scenario; thus, we take the weighted mean as an indication of a relatively short-lived glacial maximum occurring around ~8.6 kyr BP. Exposure ages of deposits at the Quartz Hills and the Caloplaca Hills show that ice had already retreated from maximum elevations by that time.

4.1.4. Hatcher Bluffs

The most recent ice thickening apparent in surface-exposure age data from Reedy Glacier is evident at Hatcher Bluffs, a nunatak at the head of the glacier (Fig. 1). A thick drape of ablation till covers the blue-ice surface that surrounds the nunatak, but only a few fresh erratics perched on a narrow, steep-sided, weathered bedrock ridge provide evidence for thicker ice in the past (Fig. 2).

Table 2
Surface-exposure ages of deposits near the head of Reedy Glacier.

Sample	Latitude (deg S)	Longitude (deg W)	Altitude (m asl)	Thickness correction	Horizon correction	[Be-10][a] (10^4 atom/g)	Exposure age[b] (kyr)	Range[c] (kyr)
Caloplaca Hills								
Reedy III limit (glacial maximum deposits; W to E)[d]								
03-RDY-135-CPH	*86.07692*	*131.22337*	*1660*	*0.957*	*0.985*	*252.8 ± 3.5*	*97.1 ± 8.7 (1.4)*	*93.9–101*
03-RDY-133-CPH	*86.07808*	*131.22262*	*1704*	*0.957*	*0.999*	*70.3 ± 1.4*	*25.3 ± 2.3 (0.5)*	*24.6–26.3*
03-RDY-117-CPH	86.08975	130.96432	1528	0.949	0.979	24.1 ± 0.9	10.2 ± 1.0 (0.4)	10.1–10.6
03-RDY-118-CPH	*86.08975*	*130.96432*	*1528*	*0.941*	*0.982*	*263.9 ± 3.9*	*115 ± 10 (2)*	*112–120*
03-RDY-128-CPH	*86.09003*	*130.96353*	*1529*	*0.945*	*0.985*	*271.7 ± 4.4*	*117 ± 11 (2)*	*114–123*
03-RDY-127-CPH	86.08998	130.95963	1525	0.945	0.986	34.7 ± 0.8	14.7 ± 1.3 (0.3)	14.5–15.4
03-RDY-124-CPH	86.08908	130.93792	1516	0.949	0.989	26.7 ± 0.6	11.3 ± 1.0 (0.3)	11.2–11.8
03-RDY-123-CPH	86.08908	130.92145	1522	0.927	0.989	24.1 ± 0.7	10.4 ± 0.9 (0.3)	10.3–10.9
03-RDY-121-CPH	*86.08825*	*130.90778*	*1517*	*0.951*	*0.992*	*105.2 ± 2.0*	*44.6 ± 4.0 (0.9)*	*43.6–46.7*
Weighted mean of samples with a simple exposure history							11.6 ± 0.2	
Mim's Spur								
Reedy III limit (glacial maximum deposits; approx. N to S along moraine)[e]								
04-RDY-168-MIM	86.04250	125.74313	1924	0.937	0.994	28.2 ± 1.4	8.8 ± 0.9 (0.4)	8.5–9.1
04-RDY-169-MIM	86.04247	125.74425	1923	0.970	0.987	28.9 ± 1.3	8.8 ± 0.9 (0.4)	8.5–9.0
04-RDY-170-MIM	86.04237	125.74607	1917	0.929	0.993	28.6 ± 1.4	9.1 ± 0.9 (0.5)	8.7–9.3
04-RDY-174-MIM	86.04386	125.70660	1988	0.970	0.992	28.8 ± 9.1	8.3 ± 2.8 (2.7)	8.0–8.5
04-RDY-174-MIM-RPT	86.04386	125.70660	1988	0.970	0.992	28.1 ± 0.7	8.1 ± 0.7 (0.2)	7.8–8.3
04-RDY-178-MIM	86.04395	125.71752	1966	0.953	0.988	29.5 ± 10.3	8.9 ± 3.2 (3.1)	8.5–9.1
04-RDY-178-MIM-RPT	86.04395	125.71752	1966	0.953	0.988	25.7 ± 0.6	7.7 ± 0.7 (0.2)	7.4–7.9
04-RDY-179-MIM	86.04405	125.71328	1970	0.953	0.989	29.8 ± 0.9	8.9 ± 0.8 (0.3)	8.5–9.1
Weighted mean							8.6 ± 0.1	
Recessional deposits (by distance below Reedy III limit)								
04-RDY-181-MIM	86.04250	125.75835	1895	0.921	0.996	23.8 ± 0.7	7.7 ± 0.7 (0.2)	7.4–7.9
04-RDY-183-MIM	*86.04262*	*125.75902*	*1892*	*0.945*	*0.994*	*52.2 ± 1.7*	*16.6 ± 1.5* (0.5)	*16–17.1*
04-RDY-186-MIM	*86.04400*	*125.80575*	*1826*	*0.961*	*0.991*	*420 ± 18*	*143 ± 14* (6)	*136–147*
Polygon Spur								
Recessional deposits (by distance from glacier margin; farthest to closest)								
04-RDY-154-PGN	*86.01080*	*126.24662*	*1654*	*0.970*	*0.999*	*56.1 ± 2.8*	*20.7 ± 2.1* (1.1)	*20.2–21.6*
04-RDY-157-PGN	86.01013	126.24988	1660	0.957	0.999	17.6 ± 1.6	6.5 ± 0.8 (0.6)	6.4–6.8
04-RDY-159-PGN	*86.01117*	*126.25185*	*1656*	*0.949*	*0.999*	*119.8 ± 2.7*	*45.3 ± 4.1* (1.0)	*44.0–47.2*
04-RDY-160-PGN	86.01145	126.25898	1657	0.953	0.994	14.1 ± 0.8	5.3 ± 0.6 (0.3)	5.2–5.5
Hatcher Bluffs								
Reedy III limit (upper limit of glacial maximum deposit on N spur)								
04-RDY-210-HCH	86.32798	126.08850	1956	0.983	0.998	25 ± 1.2	7.3 ± 0.7 (0.4)	7.0–7.5
04-RDY-211-HCH	86.32798	126.08850	1956	0.945	0.982	11.3 ± 0.7	3.5 ± 0.4 (0.2)	3.3–3.5
Weighted mean							4.8 ± 0.2	
Recessional deposits below Reedy III limit								
04-RDY-212-HCH	86.32785	126.13314	1943	0.976	0.999	15.4 ± 1.5	4.6 ± 0.6 (0.4)	4.4–4.7

Italics indicate samples assumed to have a complex exposure history.
Full CRONUS calculator input data for checking/recalculation of these results archived at: http://depts.washington.edu/cosmolab/data/.
[a] Be-10 concentrations based on Be isotopic measurements normalized to pre-2007 values of the KNSTD standard series. Multiply by 1.106 for values compatible with post-2007 normalization. See Nishiizumi et al. (2007).
[b] Simple exposure age assuming steady production rate; altitude corrections per Lal (1991) as implemented in the CRONUS calculator (http://hess.ess.washington.edu/math/). External uncertainties propagated at the $\pm 1\sigma$ level. Internal uncertainties in parentheses. See notes to Table 1.
[c] Range of exposure ages returned by the four paleomagnetically corrected production rate scaling methods implemented in the CRONUS calculator. See notes to Table 1.
[d] See location of Reedy III limit in Fig. 7.
[e] See location of Reedy III limit in Fig. 9.

An exposure age of one erratic collected from this ridge suggests that a maximum ice surface exceeded the modern ice surface by at least 50 m, at 7.3 ± 0.7 kyr BP (Table 2). A second sample from the same elevation yields a surface-exposure age of 3.5 ± 0.4 kyr BP These samples were the highest occurrence of glacially-derived material on a narrow, steep-sided, weathered bedrock ridge, which accumulated only a few, relatively unweathered erratics during the maximum. Possible explanations for these two ages include (1) two separate ice advances, or (2) a sustained maximum thickness of Reedy Glacier beginning before 7.3 kyr BP and remaining at the maximum elevation until 3.5 ± 0.4 kyr BP. We find no evidence of multiple ice advances or of a similarly-timed maximum ice thickness at other sampling locations along Reedy Glacier; results discussed in the following section indicate that a steady retreat of ice at the mouth of Reedy Glacier was underway by 7.8 ± 0.7 kyr BP.

4.2. Surface-exposure ages of recessional deposits at Reedy Glacier

Exposure ages from recessional deposits reflect two processes: retreat of the glacier margin from its maximum extent and stranding of cobbles initially exposed in till-covered ablation zones. As a result, even undisturbed samples at the same elevation can have different exposure ages. To aid interpretation, we assign recessional deposits to three groups: (I) recessional deposits with ages similar to those from the Reedy III limit are interpreted as evidence of a debris-covered, blue-ice ablation field that extended out from the margin during the glacial maximum. That is, these

Table 3
Surface-exposure ages of recessional deposits on nunataks beside lower Reedy Glacier.

Sample	Latitude (deg S)	Longitude (deg W)	Altitude (m asl)	Thickness correction	Horizon correction	[Be-10][a] (10^4 atom/g)	Exposure age[b] (kyr)	Range[c] (kyr)
Langford Peak								
Summit erratics								
04-RDY-074-LNG	85.54638	135.36480	1060	0.949	0.999	12.2 ± 0.4	7.4 ± 0.7 (0.2)	7.4–7.8
04-RDY-076-LNG	85.54642	135.37515	1050	0.957	0.997	12.5 ± 0.3	7.6 ± 0.7 (0.2)	7.6–8.1
Racine Nunatak								
Recessional deposits (by altitude)								
04-RDY-059-RCN	85.45907	136.31717	908	0.941	1.000	11.2 ± 0.3	7.8 ± 0.7 (0.2)	7.8–8.3
04-RDY-061-RCN	85.46152	136.24397	853	0.949	1.000	9.9 ± 0.3	7.2 ± 0.7 (0.2)	7.2–7.7
04-RDY-064-RCN	85.46327	136.23030	806	0.945	0.999	8.4 ± 0.3	6.4 ± 0.6 (0.2)	6.4–6.8
Pip's Peak								
Recessional deposits (by altitude)								
04-RDY-041-UNN	85.43522	135.93657	898	0.949	1.000	10.6 ± 0.3	7.4 ± 0.7 (0.2)	7.4–7.9
04-RDY-040-UNN	85.43520	135.93548	896	0.961	1.000	10.1 ± 0.2	6.9 ± 0.6 (0.2)	6.9–7.4
04-RDY-042-UNN	85.43533	135.94978	896	0.941	1.000	10.2 ± 0.2	7.2 ± 0.6 (0.2)	7.2–7.6
04-RDY-039-UNN	85.42880	135.88902	811	0.953	1.000	8.9 ± 0.3	6.7 ± 0.6 (0.2)	6.7–7.1
04-RDY-038-UNN	85.42870	135.88933	810	0.941	1.000	8.8 ± 0.2	6.7 ± 0.6 (0.2)	6.7–7.1
04-RDY-036-UNN	85.42590	135.88608	773	0.937	1.000	8.6 ± 0.2	6.7 ± 0.6 (0.2)	6.7–7.2
04-RDY-037-UNN	85.42660	135.88468	773	0.937	0.995	4.9 ± 0.1	3.9 ± 0.4 (0.1)	3.9–4.1
04-RDY-035-UNN	85.42443	135.88128	745	0.949	0.994	0.6 ± 0.1	0.51 ± 0.07 (0.06)	0.51–0.54
Cohen Nunatak								
Recessional deposits (by altitude)								
03-RDY-139-CHN	85.39980	136.22203	745	0.949	1.000	8.5 ± 0.3	6.8 ± 0.6 (0.3)	6.8–7.3
03-RDY-151-CHN	85.39982	136.21527	724	0.961	1.000	8.2 ± 0.2	6.6 ± 0.6 (0.2)	6.6–7.1
03-RDY-146-CHN	85.39970	136.19603	680	0.937	0.999	5.7 ± 0.2	4.9 ± 0.4 (0.1)	4.9–5.2
03-RDY-141-CHN	85.39973	136.18645	641	0.949	0.991	1.6 ± 0.2	1.4 ± 0.2 (0.15)	1.4–1.5
03-RDY-142-CHN	85.39973	136.18645	641	0.937	0.991	1.9 ± 0.1	1.7 ± 0.2 (0.08)	1.7–1.8
Outcrops along Reedy Glacier margin (upstream to downstream)								
04-RDY-031-BRK	85.41232	135.84777	750	0.978	1.000	0.8 ± 0.1	0.58 ± 0.08 (0.06)	0.58–0.62
04-RDY-032-BRK	85.41232	135.84782	749	0.941	1.000	0.8 ± 0.1	0.67 ± 0.07 (0.04)	0.67–0.71
04-RDY-016-SKL	85.40540	135.91125	736	0.953	1.000	4.6 ± 0.1	3.65 ± 0.34 (0.11)	3.65–3.91
04-RDY-015-SKL	85.40537	135.91193	735	0.987	1.000	4.7 ± 0.2	3.61 ± 0.34 (0.12)	3.61–3.87
04-RDY-022-SKL-RPT	85.40572	135.86155	728	0.949	0.998	1.0 ± 0.1	0.82 ± 0.10 (0.06)	0.82–0.88
04-RDY-003-JGN	85.38615	136.27515	633	0.933	0.992	0.6 ± 0.1	0.52 ± 0.07 (0.05)	0.52–0.56
"Drifting" (blue-ice) moraines near Cohen Nunatak								
04-RDY-068-DRM	85.38845	136.19483	637	0.949	0.999	0.3 ± 0	0.28 ± 0.05 (0.04)	0.28–0.30
04-RDY-070-DRM	85.39452	136.19140	631	0.945	0.999	0.4 ± 0.1	0.32 ± 0.05 (0.05)	0.32–0.34
03-RDY-153-CHN	85.41313	136.23483	587	0.949	1.000	0.2 ± 0	0.22 ± 0.04 (0.03)	0.22–0.24
03-RDY-154-CHN	85.41313	136.23483	587	0.949	1.000	0.1 ± 0	0.13 ± 0.03 (0.03)	0.13–0.14

Full CRONUS calculator input data for checking/recalculation of these results archived at: http://depts.washington.edu/cosmolab/data/.
[a] Be-10 concentrations based on Be isotopic measurements normalized to pre-2007 values of the KNSTD standard series. Multiply by 1.106 for values compatible with post-2007 normalization. See Nishiizumi et al. (2007).
[b] Simple exposure age assuming steady production rate; altitude corrections per Lal (1991) as implemented in the CRONUS calculator (http://hess.ess.washington.edu/math/). External uncertainties propagated at the ±1σ level. Internal uncertainties in parentheses. See notes to Table 1.
[c] Range of exposure ages returned by the four paleomagnetically corrected production rate scaling methods implemented in the CRONUS calculator. See notes to Table 1.

erratics were exposed on the ice surface during the glacial maximum, but were not deposited until ice beneath them sublimed away, stranding them at a range of altitudes; (II) samples with ages younger than the time of the glacial maximum became exposed after the glacier had begun thinning; these also may span a wide range of ages because material may have been stranded on slowly thinning ablation fields; (III) as discussed previously, we assume that samples with exposure ages that greatly exceed the time of the glacial maximum are recycled, having been exposed previously in older deposits. We assume all other ages are essentially correct and have not been affected by post-depositional processes. If one accepts this, as well as the interpretation of the three groups, then ages in the second group constrain the timing of retreat from the maximum position. That is, samples with the *youngest* surface-exposure ages at a given elevation set a maximum limit on ice thickness at that time. Likewise, the *highest* erratic of a given age sets a minimum limit on the ice thickness.

4.2.1. Quartz Hills

We analyzed 24 erratics from recessional deposits below the Reedy III limit in the Quartz Hills; 20 samples were collected from the north slope leading to the bench, and four were collected from the bluff that overlooks the glacier (Fig. 3; Table 1). Of the twenty-four recessional samples, three fall within the range of the glacial maximum (17.0–14.1 kyr BP); we interpret these as Group I samples. Five samples greatly exceed the timing of maximum ice thickness; we interpret these as Group III samples. The ages and elevations of the other 16 samples (Group II) afford constraints on the maximum and minimum elevations of the glacier at given times (Fig. 6). Results indicate that thinning was underway by ~13 kyr BP, the age of the oldest recessional sample younger than the age range found at the maximum elevation. The maximum elevation of the ice margin decreased from ~1400 m asl at 14.1 kyr BP to 1310 m by 9 kyr BP, to 1270 m by 7.0 kyr BP. Further, the lack of exposure ages younger than 7.0 kyr BP at elevations above 1272 m asl suggests that the glacier had thinned by ~130 m between 14.1 kyr BP and 7.0 kyr BP. This

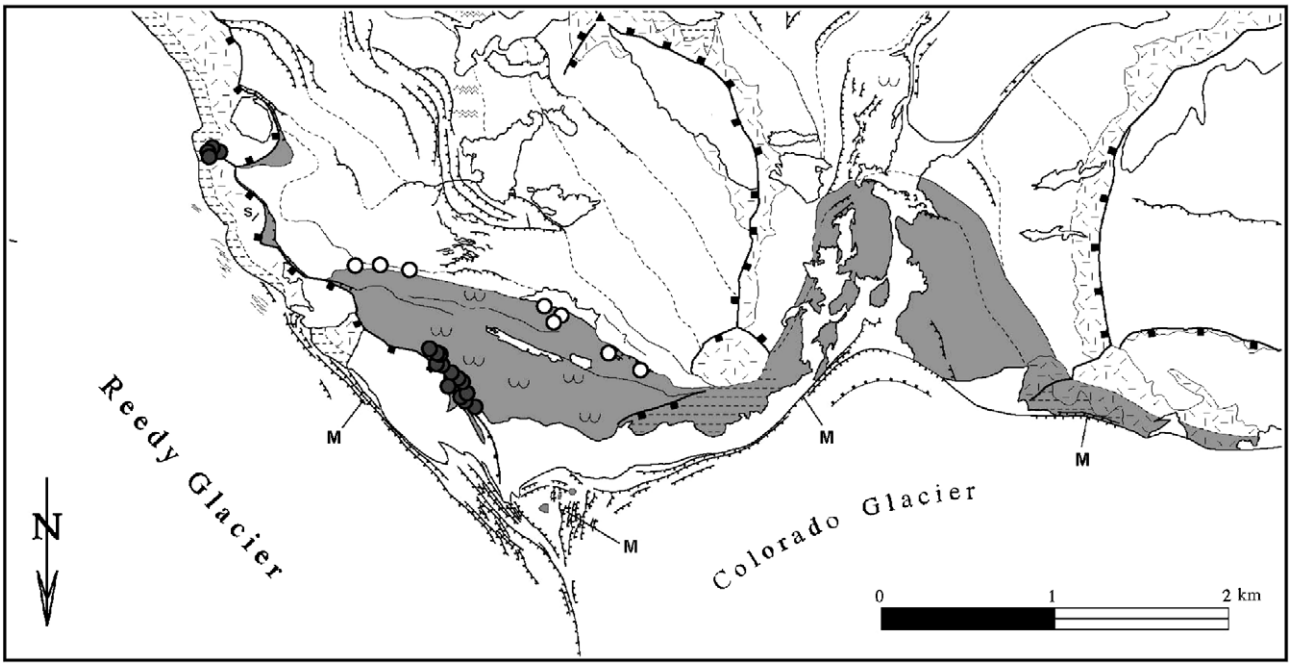

Fig. 5. Glacial geologic map of the Quartz Hills from Bromley et al. (2010). Shaded areas indicate the extent of the Reedy III deposit. White circles show location of samples from the upper limit of the Reedy III deposit. Dark gray circles show location of samples from recessional deposits. Glacial geologic mapping is explained in greater detail by Bromley et al. (2010).

amounts to ~130 m in 7.1 kyr, or an average thinning rate of ~20 cm/yr.

4.2.2. Lower Reedy Glacier

During the last glaciation Reedy Glacier overran peaks at its mouth and there is no record of its maximum thickness there. Deposits on these peaks date from the time of ice retreat. Langford Peak (1060 m asl), located 43 km down-glacier from the Quartz Hills and ~25 km from the mouth emerged 7.5 ± 0.5 kyr BP (Table 3). Exposure ages of samples from nunataks closer to the confluence of Reedy Glacier and Mercer Ice Stream, all indicate that their summits emerged at about the same time: Racine Nunatak (853 m asl) emerged 7.8 ± 0.7 kyr BP; Pip's Peak (898 m asl) emerged by 7.2 ± 0.4 kyr BP (mean age of three summit erratics); Cohen Nunatak (745 m asl) emerged by 6.8 ± 0.6 kyr BP (Table 3).

Erratics lower on these peaks have younger ages. However, interpreting the thinning history of Reedy Glacier from these data is complicated because the peaks are set back different distances from its margin (e.g., Racine Nunatak is 6 km, and Cohen Nunatak 2 km from the glacier edge). Two of these peaks, Racine Nunatak and Pip's Peak, emerged fully in 1–3 kyr after their summits emerged (Table 3). Cohen Nunatak, which is now isolated from the main glacier by a bedrock ridge that outcrops as a string of low knolls along the glacier margin (Fig. 4), emerged more slowly. Ice here thinned from 745 m asl at 6.8 kyr BP, to 680 m at 4.9 kyr BP, to 640 m (the base of the nunatak) by 1.5 kyr BP (Table 3). Erratics from the low bedrock outcrops along the modern glacier margin are generally much younger (~500–800 yrs BP) than those on the main peaks. Exceptions are two erratics collected from a small knoll just 30 m above the crevassed glacier margin that have been exposed for 3.6 kyr. It is possible that these erratics spent considerable time on the glacier surface in a local blue-ice moraine field before being deposited. However, 4 clasts from two nearby patches of "drifting" ablation till have been exposed for much less time, ranging from 130 to 320 (±30–50) years. In addition, we suspect that some of the complexity in these data is due to the complicated bed topography of this area which likely pinned and obstructed migration of the glacier margin as flow contracted into the present trough.

4.2.3. Polygon Spur

We collected four fresh erratics from a broad, undulating bedrock bench at Polygon Spur (Fig. 2), approximately 30 m above the closest ice margin (we note however, that the margin rises and falls by more than 120 m elsewhere around the periphery of Polygon Spur, and it is therefore difficult to infer changes in the thickness of the adjacent glaciers from these samples). The samples were collected from within a diffuse deposit of unweathered erratics with a poorly defined outer margin (Bromley et al., 2010), but we assume that these erratics were exposed as ice retreated across the bench from its maximum extent. Two of the four erratics yielded ages of 6.5 ± 0.8 kyr and 5.3 ± 0.6 kyr BP (Table 2), which are consistent with evidence that retreat from the maximum ice thickness at adjoining Mims Spur occurred after 7.7 ± 0.7 kyr BP The remaining two erratics yielded much older ages, and thus are presumed to have been previously exposed (Group III).

4.2.4. Mims Spur

Two of three samples from recessional deposits at Mims Spur fall into Group III, with surface-exposure ages of 16.6 ± 1.5, and 143 ± 14 kyr BP, which exceed the age of maximum ice thickness at this location (Table 2). The third sample yielded an age of 7.7 ± 0.7 kyr BP, which cannot be distinguished from the age of the maximum. We interpret this result as a Group II recessional deposit. Thus, available data from Mims Spur suggest that the glacier surface there has thinned about 140 m since 7.7 kyr BP, but results from the recessional samples do not constrain the thinning history. As noted above, two recessional samples from Polygon Spur suggest that the nearby glacier margin had dropped to within 30 m

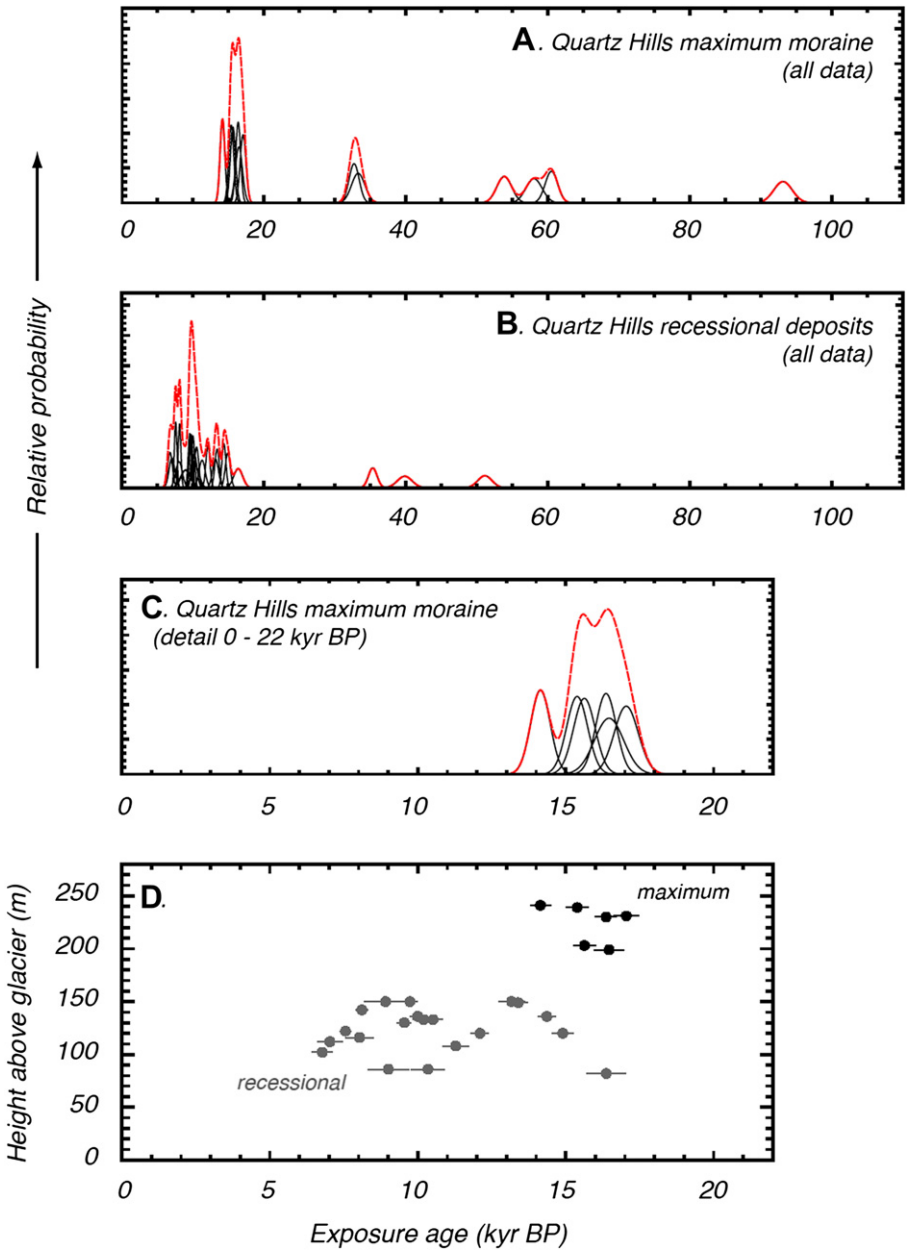

Fig. 6. A – C) Probability density functions of surface-exposure age results from erratics collected from the maximum moraine in the Quartz Hills (at the upper limit of the Reedy III deposit), and from recessional deposits below the upper limit of the Reedy III deposit. Each exposure age and its internal uncertainty are represented by a small Gaussian curve. Dashed line represents the total probability density function of all samples reported in each panel (see footnote to Table 1). D) Surface-exposure ages from the maximum moraine and from recessional deposits in the Quartz Hills, plotted by altitude of sample. Exposure ages indicative of prior exposure are not included.

of its present elevation by 5.3 kyr BP. It is possible that these changes reflect localised adjustments of the complex ice margin surrounding Polygon and Mims Spurs. Alternatively, they suggest that deglaciation of Polygon Spur occurred rapidly and that much of the area had been exposed by ~6 kyr BP.

4.2.5. Hatcher Bluffs

At Hatcher Bluffs, a sample 13 m below the Reedy III upper limit dates to 4.6 ± 0.6 kyr BP (Table 2) within the range established for the upper limit (7.3–3.5 kyr BP). We infer that it was exposed at the ice surface during the glacial maximum, but did not reach the ice margin (a Group I type deposit); it was not deposited until after the glacier thinned by 13 m. Our data indicate that the glacier surface at Hatcher Bluffs has thinned about 50 m in the past 3.5 kyr.

5. Discussion

5.1. Evolution of glacier profile

Our spatially distributed exposure ages indicate that the timing of the glacial maximum along the length of Reedy Glacier was not synchronous. From dates at the Quartz Hills, located about halfway up the glacier, we infer the maximum limit was reached by 17 kyr BP and persisted until at least 14 kyr BP This is the earliest recorded maximum at Reedy Glacier. Farther upstream, the glacier remained at its maximum thickness until more recently. We assume the cluster of ages from the Caloplaca Hills (14.7–10.2 kyr BP; Table 2) represents the age and minimum duration of thicker ice at that site. At Mims Spur, the Reedy III maximum limit

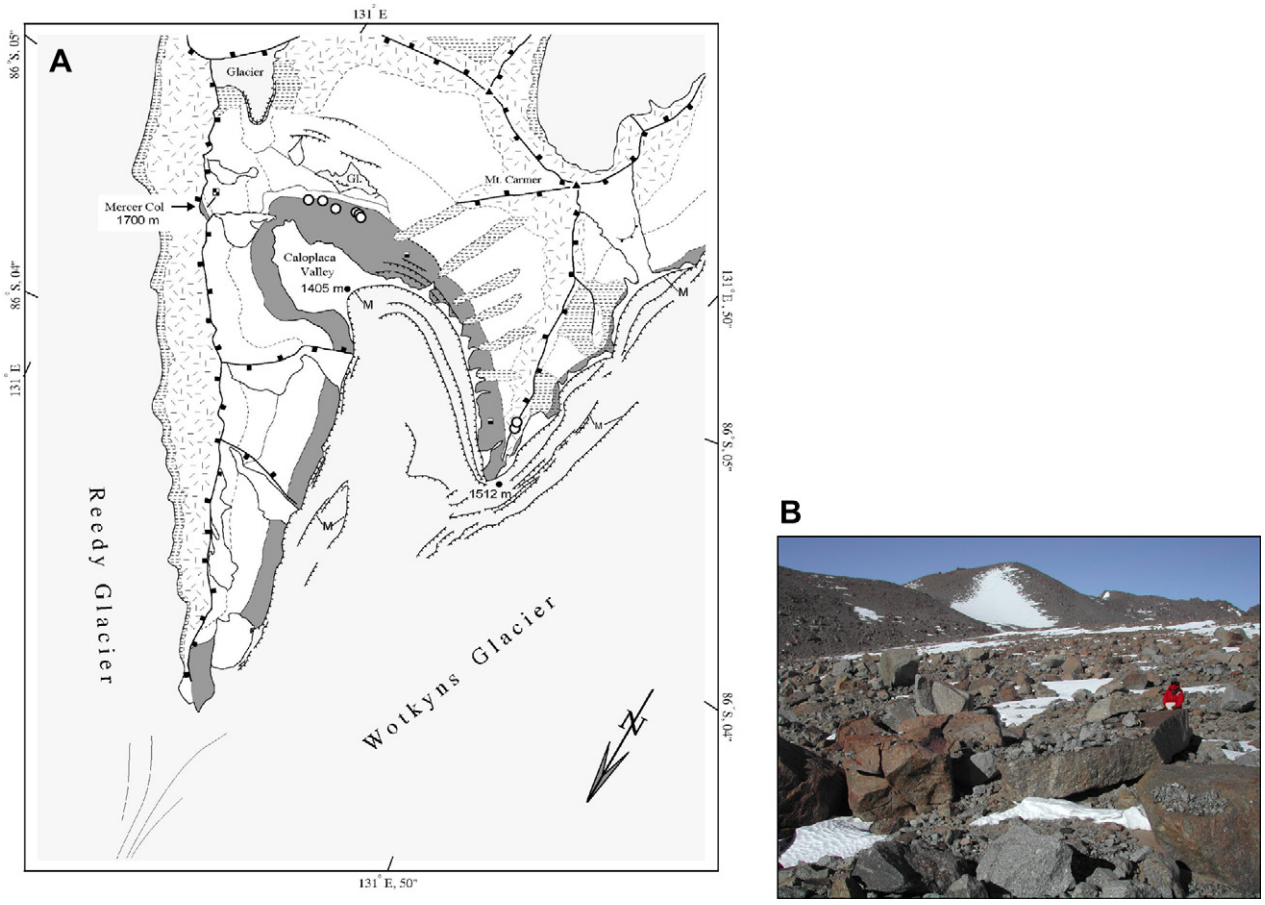

Fig. 7. A) Glacial geologic map of the Caloplaca Hills from Bromley et al. (2010). Shaded areas indicate the extent of the Reedy III deposit. White circles show location of samples from the upper limit of the Reedy III deposit. Glacial geologic mapping is explained in greater detail by Bromley et al. (2010). B) Unweathered erratics perched on embedded, weathered boulders at the upper limit of the Reedy III deposit in the Caloplaca Hills.

was reached by 9.1 kyr BP and ice remained there until at least 7.7 kyr BP At Hatcher Bluffs a single exposure age indicates that the ice surface there was near its maximum at 7.3 kyr BP. A second sample suggests that ice may have remained at this elevation until 3.5 kyr BP (Table 2). Although it is possible that older erratics dating to the Quartz Hills maximum were not sampled at the locations upstream, the clustering of exposure ages from Reedy III deposits at Caloplaca Hills and especially at Mims Spur suggest that this was

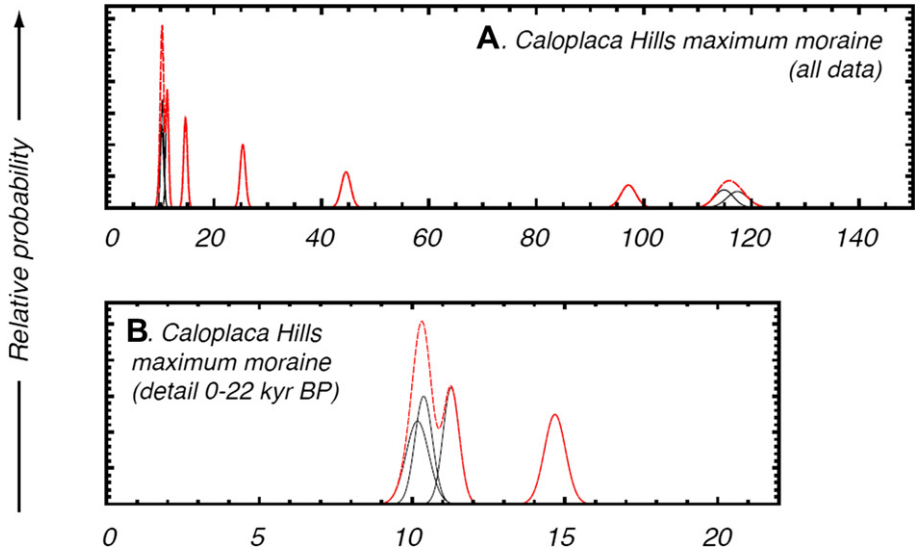

Fig. 8. A – B) Probability density functions of surface-exposure age results from erratics collected from the maximum moraine in the Caloplaca Hills (at the upper limit of the Reedy III deposit). Each exposure age and its internal uncertainty are represented by a small Gaussian curve. Dashed line represents the total probability density function of all samples reported in each panel (see footnote to Table 1).

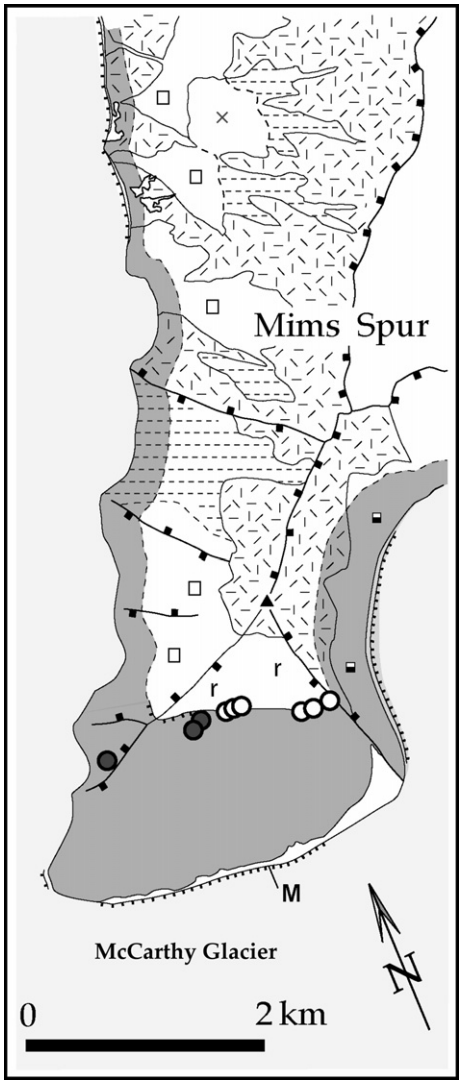

Fig. 9. Glacial geologic map of Mims Spur from Bromley et al. (2010). Shaded areas indicate the extent of the Reedy III deposit. White circles show location of samples from the upper limit of the Reedy III deposit. Dark gray circles show location of samples from recessional deposits. Glacial geologic mapping is explained in greater detail by Bromley et al. (2010).

not the case. Another possibility is that an advance of Olentangy and McCarthy Glaciers caused localised thickening at Mims Spur unrelated to Reedy Glacier downstream, but this seems unlikely because of the proximity of Mims Spur to Reedy Glacier (20 km) and the fact that these glaciers share similar and adjacent accumulation areas on the polar plateau.

Our leading hypothesis is that thickening started near the mouth of the Reedy Glacier in response to buttressing of flow from grounded ice in the Ross Sea, which caused a wave of thickening to propagate upstream. Likewise, a wave of thinning would propagate up-glacier as grounded ice in the Ross Embayment retreated and thinned. Following this hypothesis, we interpret the high-stand at the Quartz Hills as evidence that buttressing near the mouth started prior to 17 kyr BP, and the onset of deglaciation at the Quartz Hills 13 kyr BP as evidence that the Ross Sea ice sheet was thinning by that time. In contrast, thickening up-glacier continued long after deglaciation was underway in the Quartz Hills. We attribute this apparent thickening during the early-mid Holocene to be a response to increased snow accumulation in East Antarctica (Lorius et al., 1985; Petit et al., 1999). A transient ice-flow model of the Reedy Glacier with realistic boundary conditions is needed to fully test this conceptual model, however ice-sheet models (e.g., Ackert et al., 2007) consistently show maximum elevations near the ice divide were reached in the early Holocene.

5.2. Thickness of last glacial maximum ice in the southeastern Ross Embayment

Our data place new constraints on the thickness of the Ross Ice Sheet in the southeastern corner of the Ross Embayment during the last glacial maximum in the region. Although we cannot constrain the pattern of ice-stream drainage beyond the mouth of Reedy Glacier, we can establish that the *maximum possible* elevation of the ice sheet was 1400 m (the elevation of maximum ice thickness at the Quartz Hills). The summit of Langford Peak (1060 m asl) emerged at 7.5 kyr BP when ice at the Quartz Hills, 43 km farther up-glacier stood at ~1280 m (Tables 1 and 3); hence the surface slope of the lower reaches of the glacier at that time was ~0.005. Comparison with the modern slope (0.0079) shows that the surface profile was less steep during the glacial maximum, and became steeper during deglaciation (Denton and Hughes, 2000). It is likely that the surface slope was shallower than that 7.5 kyr ago, midway through deglaciation, but we use this slope to estimate a *minimum* local glacial maximum elevation at the glacier mouth of 1060 m asl.

Our bracketing range for the elevation of ice near the mouth of Reedy Glacier during the glacial maximum (1060–1400 m asl) is lower than the value of 1700 m asl used in reconstructions by Denton and Hughes (2002) and Huybrechts (2002), indicating that these models overestimate the volume of Ross Sea ice and its contribution to global sea-level change. However, our surface elevations are higher than the reconstruction of Mercer Ice Stream during the last glacial maximum presented by Ackert et al. (2007); it is possible that the value they used to parameterize the basal traction for Mercer Ice Stream is too small. Increased basal traction would cause discharge from Mercer Ice Stream to slow and ice-surface elevations to increase. Our data indicate that the Ross Ice Sheet downstream of Reedy Glacier was 450–800 m thicker during the last glaciation than present-day ice at the glacier mouth. The timing of the glacial maximum recorded at the Quartz Hills (17.0–14.1 kyr BP) is consistent with data for maximum ice extent from farther north in the Transantarctic Mountains and Ross Sea (e.g., Bockheim et al., 1989; Licht et al., 1996; Hall and Denton, 2000; Licht and Andrews, 2002).

5.3. Deglaciation of the southeastern Ross Embayment

Exposure ages from the Quartz Hills indicate that deglaciation of the lower reaches of Reedy Glacier was underway by 13 kyr BP, similar to the timing of initial ice-thinning farther north (Bockheim et al., 1989; Hall and Denton, 2000). This is similar to model results that indicate Siple Dome thinned ~350 m sometime between 15 and 10 kyr BP (Price et al., 2007) and models that suggest increased ice-stream discharge and thinning in response to post-glacial warming was delayed until about 13 kyr BP (Parizek et al., 2003).

However, unlike Siple Dome, thinning of Reedy Glacier continued through the Holocene. Ice-elevations near the glacier mouth decreased ~100 m after 7 kyr BP. The average rate of thinning over the past 1000 years has been less than 0.02 m/yr. Exposure ages show that outcrops 5–40 m above the glacier surface in the present shear margin were uncovered within the past 500–800 years, indicating continued slow thinning of the region.

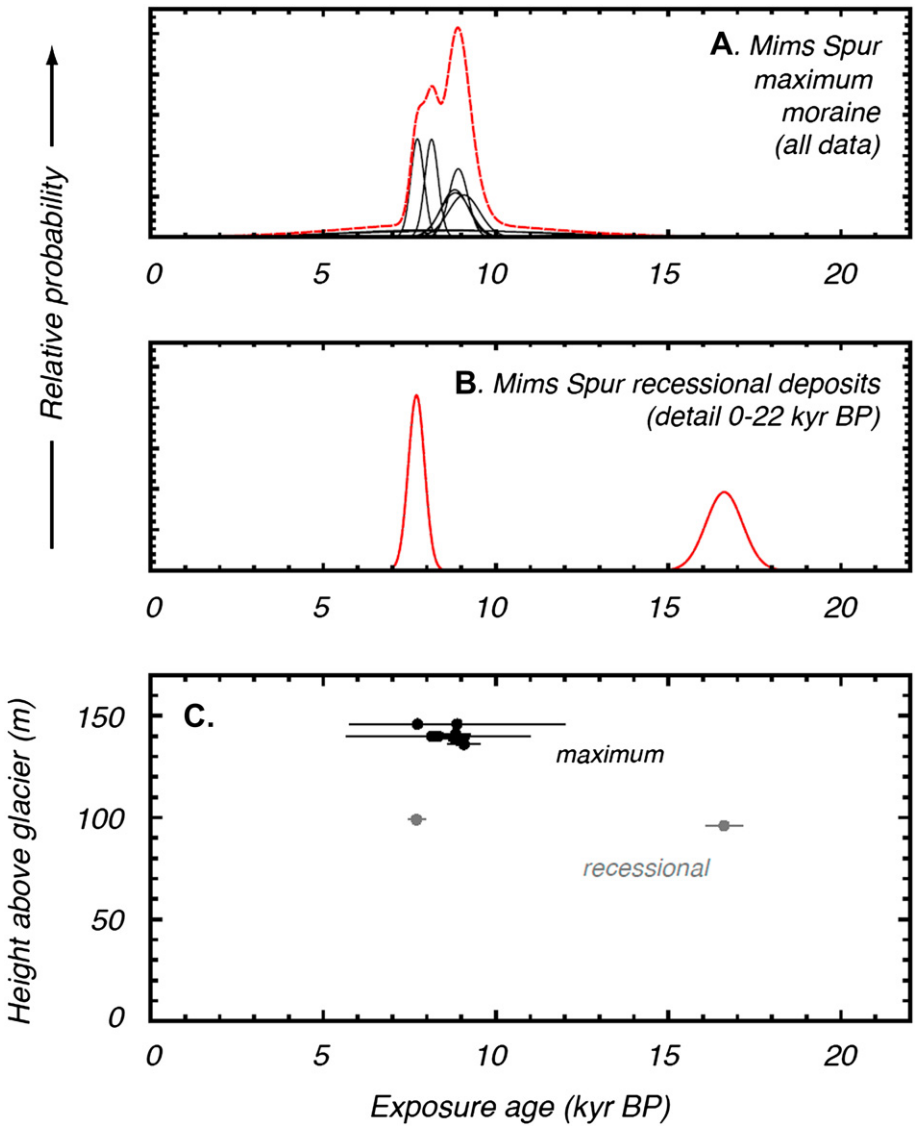

Fig. 10. A – B) Probability density functions of surface-exposure age results from erratics collected from the maximum moraine at Mims Spur (at the upper limit of the Reedy III deposit), and from recessional deposits below the upper limit of the Reedy III deposit. Each exposure age and its internal uncertainty are represented by a small Gaussian curve. Dashed line represents the total probability density function of all samples reported in each panel (see footnote to Table 1). C) Surface-exposure ages from the maximum moraine and from recessional deposits at Mims Spur, plotted by altitude of sample. Exposure ages indicative of prior exposure are not included.

6. Conclusions

We dated both the maximum and recessional positions of Reedy Glacier following the LGM. Exposure ages show that the maximum position was not synchronous along the glacier. The maximum at the Quartz Hills was reached by 17.0 kyr BP and persisted until at least 14.1 kyr BP Thinning was underway at Quartz Hills by 13 kyr BP In contrast, farther up-glacier ice was still thickening at this time. We attribute this asynchronous behavior along the glacier to the effects of two different processes. At the glacier mouth, growth and subsequent deglaciation of the Ross Sea ice sheet caused a wave of thickening and then thinning to propagate up-glacier. The response to forcing at the mouth was delayed and attenuated at the head of the glacier, but postglacial increase of accumulation in East Antarctica increased the flux of ice into the upper reaches of the glacier, causing transient thickening at the glacier head. Our data suggest that the glacier did not attain equilibrium during the last glaciation.

Our results constrain the thickness of grounded ice in the southeastern corner of the Ross Sea during the last local glacial maximum to within the range of 1060–1400 m asl, with the lower end of the estimate resulting from use of a surface profile dropping steeply from the Quartz Hills, and the upper limit results from use of a flat glacier surface extending from the Quartz Hill**s**. This maximum was reached in the Quartz Hills at 17.0–14.1 kyr BP, timing which is consistent with dates from other sites in the Ross Embayment. The reconstructed surface elevation, however, is several hundred meters lower than used in some recent regional LGM models for this part of Antarctica. Deglaciation of the lower reaches of Reedy Glacier was underway by 13 kyr BP At its confluence with Mercer Ice Stream the glacier has thinned by less than 20 m in the past 1000 years.

Acknowledgements

This work was funded by grants from the Office of Polar Programs, US National Science Foundation (OPP-0229314 and OPP-

0229034). We thank M. Conway for assistance in the field, UNAVCO for assistance with GPS data, and Raytheon Polar Services, the Air National Guard and Kenn Borek Air for transportation and logistical support. Joy Laydbak helped with sample preparation. We also thank Marc Caffee, Bob Finkel and others at PRIME Lab and LLNL-CAMS who provided high quality AMS analyses. We are also grateful for two anonymous reviews that provided thoughtful, thorough advice for improving this manuscript.

References

Ackert, R.P., Mukhopadhyay, S., Parizek, B.R., Borns, H.W., 2007. Ice elevation near the West Antarctic Ice Sheet divide during the Last Glaciation. Geophysical Research Letters 34, L21506. doi:10.1029/2007GL031412.

Anderson, J.B., Shipp, S.S., Bartek, L.R., Reid, D.E., 1992. Evidence for a grounded ice sheet on the Ross Sea continental shelf during the late Pleistocene and preliminary palaeodrainage reconstructionContributions to Antarctic Research III. Antarctic Research Series 57, 39–62.

Balco, G., Stone, J.O., Lifton, N.A., Dunai, T.J., 2008. A complete and easily accessible means of calculating surface exposure ages or erosion rates from ^{10}Be and ^{26}Al measurements. Quaternary Geochronology 3, 174–195.

Baroni, C., Hall, B., 2004. A new relative sea-level curve for Terra Nova Bay, Victoria Land, Antarctica. Journal of Quaternary Science 19, 377–396.

Bockheim, J.G., Wilson, S.C., Denton, G.H., Anderson, B.G., Stuiver, M., 1989. Late Quaternary fluctuations of Hatherton Glacier, Transantarctic Mountains. Quaternary Research 31, 229–254.

Bromley, G.R.M., Hall, B.L., Stone, J.O., Conway, H., Todd, C.E., 2010. Cenozoic deposits at Reedy Glacier, Transantarctic Mountains: implications for former thickness of the West Antarctic Ice Sheet. Quaternary Science Reviews 29, 384–398.

Brown, E.T., Edmond, J.M., Raisbeck, G.M., Yiou, F., Kurz, M.D., Brook, E.J., 1991. Examination of surface exposure ages of Antarctic moraines using in situ produced ^{10}Be and ^{26}Al. Geochimica et Cosmochimica Acta 55, 2269–2283.

Chinn, T.J., 1994. Glacier disequilibrium in the Convoy Range, Transantarctic Mountains, Antarctica. Annals of Glaciology 20, 269–276.

Conway, H., Hall, B.L., Denton, G.H., Gades, A.M., Waddington, E.D., 1999. Past and future grounding-line retreat of the West Antarctic Ice Sheet. Science 286, 280–283.

Denton, G.H., Bockheim, J.G., Wilson, S.C., Leide, J.E., Andersen, B., 1989. Late Quaternary ice-surface fluctuations of Beardmore Glacier, Transantarctic Mountains. Quaternary Research 31, 183–209.

Denton, G.H., Hughes, T.J., 2002. Reconstructing the Antarctic Ice Sheet at the last glacial maximum. Quaternary Science Reviews 21, 193–202.

Denton, G.H., Hughes, T.J., 2000. Reconstruction of the Ross ice drainage system, Antarctica, at the last glacial maximum. Geografiska Annaler 82 A, 143–166.

Ditchburn, R.G., Whitehead, N.E., 1994. The separation of 10Be from silicates. 3d Workshop of the South Pacific Environmental Radioactivity Association, pp. 4–7.

Gosse, J.C., Phillips, F.M., 2001. Terrestrial in-situ cosmogenic nuclides: theory and application. Quaternary Science Reviews 20, 1475–1560.

Hall, B., Baroni, C., Denton, G., 2004. Holocene relative sea-level history of the southern Victoria Land coast, Antarctica. Global and Planetary Change 42, 241–263.

Hall, B.L., Denton, G.H., 2000. Radiocarbon chronology of Ross Sea drift, eastern Taylor Valley, Antarctica: evidence for a grounded ice sheet in the Ross Sea at the last glacial maximum. Geografiska Annaler 82A, 305–336.

Huybrechts, P., 2002. Sea-level changes at the LGM from ice-dynamic reconstructions of the Greenland and Antarctic ice sheets during the glacial cycles. Quaternary Science Reviews 21, 203–231.

Joughin, I., Tulaczyk, S., 2002. Positive mass balance of the Ross Ice Streams, West Antarctica. Science 295, 476–480.

Kavanaugh, K.L, Cuffey, K.M., Morse, D.L., Conway, H., Rignot, E., 2009. Dynamics and mass balance of Taylor Glacier, Antarctica: 1. Geometry and surface velocities. Journal of Geophysical Research 114, doi:10.1029/2009JF001309.

Kohl, C.P., Nishiizumi, K., 1992. Chemical isolation of quartz for measurement of in-situ-produced cosmogenic nuclides. Geochimica et Cosmochimica Acta 56, 3583–3587.

Lal, D., 1991. Cosmic ray labeling of erosion surfaces: in situ nuclide production rates and erosion models. Earth and Planetary Science Letters 104, 424–439.

Licht, K.J., Jennings, A.E., Andrews, J.T., Williams, K.M., 1996. Chronology of late Wisconsin ice retreat from the western Ross Sea, Antarctica. Geology 24, 223–226.

Licht, K.J., Andrews, J.T., 2002. The ^{14}C record of Late Pleistocene ice advance and retreat in the central Ross Sea, Antarctica. Arctic, Antarctic and Alpine Research 34, 324–333.

Liu, H.X., Jezek, K.C., Li, B., Zhao, Z., 2001. Radarsat Antarctic Mapping Project Digital Elevation Model Version 2. National Snow and Ice Data Center, Boulder, CO. Digital Media.

Lorius, C., Jouzel, J., Ritz, C., Merlvat, L., Barkov, N., Korotkevitch, Y., Kotlyakov, V., 1985. A 150,000-year climatic record from Antarctic ice. Nature 316, 591–596.

Mayewski, P., 1975. Glacial Geology and Late Cenozoic History of the Transantarctic Mountains, Antarctica. Institute of Polar Studies, Ohio State, Report 56, p. 168.

Mercer, J.H., 1968. Glacial geology of the Reedy Glacier area, Antarctica. Geological Society of America Bulletin 79, 471–486.

Nishiizumi, K., Kohl, C.P., Klein, J., Middleton, R., Lal, D., Arnold, J.R., 1991. Cosmic ray produced ^{10}Be and ^{26}Al in Antarctic rocks: exposure and erosion history. Earth and Planetary Science Letters 104, 440–454.

Nishiizumi, K., Imamura, M., Caffee, M.W., Southon, J.R., Finkel, R.C., McAninch, J., 2007. Absolute calibration of Be-10 AMS standards. Nuclear Instruments and Methods in Physics Research B 258, 403–413.

Oliver, R.L., 1964. The level of former glaciation near the mouth of Beardmore Glacier. In: Adie, R.J. (Ed.), Antarctic Geology. North-Holland, pp. 248–258.

Orombelli, G., Baroni, C., Denton, G.H., 1990. Late Cenozoic glacial history of the Terra Nova Bay region, northern Victoria Land, Antarctica. Geografica Fisica e Dinamica Quaternaria 13, 139–163.

Parizek, B.R., Alley, R.B., Hulbe, C.L., 2003. Subglacial thermal balance permits ongoing grounding-line retreat along Siple Coast of West Antarctica. Annals of Glaciology 36, 251–256.

Petit, J.R., Jouzel, J., Raynaud, D., Barkov, N.I., Barnola, J.-M., Basile, I., Bender, M., Chappellaz, J., Davis, M., Delaygue, G., Delmotte, M., Kotlyakov, V.M., Legrand, M., Lipenkov, V.Y., Lorius, C., Pepin, L., Ritz, C., Saltzman, E., Stievenard, M., 1999. Climate and atmospheric history of the past 420,000 years from the Vostok ice core, Antarctica. Nature 399, 429–436.

Price, S.F., Conway, H., Waddington, E.D., 2007. Evidence for late Pleistocene thinning of Siple Dome, West Antarctica. Journal of Geophysical Research 112. doi:10.1029/2006JF000725.

Robinson, P.H., 1984. Ice dynamics and thermal regime of Taylor Glacier, South Victoria Land, Antarctica. Journal of Glaciology 30, 153–160.

SCAR, 2002. Antarctic Digital Database. Scientific Committee on Antarctic Research. http://www.nerc-bas.ac.uk/public/magic/add_home.html Digital data.

Shipp, S., Anderson, J.B., Domack, E.W., 1999. Late Pleistocene-Holocene retreat of the West Antarctic ice-sheet system in the Ross Sea; Part 1, Geophysical results. Geological Society of America Bulletin 111, 1486–1516.

Staiger, J., Gosse, J., Toracinta, R., Oglesby, B., Fastook, J., Johnson, J.V., 2007. Atmospheric scaling of cosmogenic nuclide production: climate effect. Journal of Geophysical Research B 112, B02205. doi:10.1029/2005JB003811.

Stone, J., Balco, G., Sugden, D., Caffee, M., Sass, L., Cowdery, S., Siddoway, C., 2003. Holocene deglaciation of Marie Byrd Land, West Antarctica. Science 299, 99–102.

Stone, J., 2000. Air pressure and cosmogenic isotope production. Journal of Geophysical Research 105, 23753–23759.

Stone, J.O., members of the UW Cosmogenic Nuclide Research Group, 2001. Extraction of Al and Be from quartz for isotopic analysis. http://depts.washington.edu/cosmolab/chem/Al-26_Be-10.pdf.

Stuiver, M., Denton, G.H., Hughes, T.J., Fastook, J.L., 1981. History of the marine ice sheet in West Antarctica during the last glaciation: a working hypothesis. In: Denton, G.H., Hughes, T.J. (Eds.), The Last Great Ice Sheets. Wiley-Interscience, New York, pp. 319–436.

Sugden, D.E., Balco, G., Cowdery, S.G., Stone, J.O., Sass, L.C., 2005. Selective glacial erosion and weathering zones in the coastal mountains of Marie Byrd Land, Antarctica. Geomorphology 67, 317–334.